THE JOURNAL OF BIOLOGICAL CHEMISTRY VOL. 285, NO. 23, pp. 17896–17906, June 4, 2010
Printed in the U.S.A.

TPPP/p25 Promotes Tubulin Acetylation by Inhibiting Histone Deacetylase 6*

Received for publication, December 18, 2009, and in revised form, March 12, 2010 Published, JBC Papers in Press, March 22, 2010, DOI 10.1074/jbc.M109.096578

Natália Tőkési[‡], Attila Lehotzky[‡], István Horváth[‡], Bálint Szabó[§], Judit Oláh[‡], Pierre Lau[¶], and Judit Ovádi[‡1]

From the [‡]Institute of Enzymology, Biological Research Center, Hungarian Academy of Sciences, Karolina u. 29., H-1113, Budapest, Hungary, the [§]Department of Biological Physics, Eötvös Loránd University, Pázmány Péter Sétány 1/A, H-1117 Budapest, Hungary, and the [¶]Section of Developmental Genetics, NINDS, National Institutes of Health, Bethesda, Maryland 20892

TPPP/p25 (tubulin polymerization-promoting protein/p25) is an unstructured protein that induces microtubule polymerization *in vitro* and is aligned along the microtubule network in transfected mammalian cells. In normal human brain, TPPP/p25 is expressed predominantly in oligodendrocytes, where its expression is proved to be crucial for their differentiation process. Here we demonstrated that the expression of TPPP/p25 in HeLa cells, in doxycycline-inducible CHO10 cells, and in the oligodendrocyte CG-4 cells promoted the acetylation of α-tubulin at residue Lys-40, whereas its down-regulation by specific small interfering RNA in CG-4 cells or by the withdrawal of doxycycline from CHO10 cells decreased the acetylation level of α-tubulin. Our results indicate that TPPP/p25 binds to HDAC6 (histone deacetylase 6), an enzyme responsible for tubulin deacetylation. Moreover, we demonstrated that the direct interaction of these two proteins resulted in the inhibition of the deacetylase activity of HDAC6. The measurement of HDAC6 activity showed that TPPP/p25 is able to induce almost complete (90%) inhibition at 3 μM concentration. In addition, treatment of the cells with nocodazole, vinblastine, or cold exposure revealed that microtubule acetylation induced by trichostatin A, a well known HDAC6 inhibitor, does not cause microtubule stabilization. In contrast, the microtubule bundling activity of TPPP/p25 was able to protect the microtubules from depolymerization. Finally, we demonstrated that, similarly to other HDAC6 inhibitors, TPPP/p25 influences the microtubule dynamics by decreasing the growth velocity of the microtubule plus ends and also affects cell motility as demonstrated by time lapse video experiments. Thus, we suggest that TPPP/p25 is a multiple effector of the microtubule organization.

TPPP/p25 (tubulin polymerization-promoting protein/p25) is an unstructured protein, originally identified in oligodendrocytes and considered as brain-specific (1, 2). However, its occurrence in ciliary structures has been recently reported (3). This protein is a new marker for synucleinopathies (4). In pathological conditions, TPPP/p25 is enriched in filamentous α-synuclein-bearing Lewy bodies of Parkinson disease (PD)[2] and diffuse Lewy body disease (5) as well as in glial cytoplasmic inclusions from multiple system atrophy brain tissues (6). TPPP/p25 polymerizes tubulin *in vitro* into normal and aberrant microtubules depending on its concentration and its phosphorylation state (7, 8). When expressed at low level in transfected HeLa cells, TPPP/p25 colocalizes specifically with the microtubules and induces microtubule bundling (9). This colocalization along the microtubules is dynamic, as demonstrated by fluorescence recovery after photobleaching experiments (9). However, a high expression level of TPPP/p25 induces aberrant microtubule ultrastructures, such as perinuclear cages and aggresomes, which mimic the formation of pathological brain inclusions (9). Our studies on primary oligodendrocytes and on the CG-4 oligodendrocyte cell line demonstrated that TPPP/p25 expression is crucial for their differentiation process, probably via a role in the rearrangement of the microtubule network during the process elongation prior to the onset of myelination (10). The down-regulation of TPPP/p25 by using TPPP/p25 siRNA or by overexpressing a specific microRNA (miR-206) resulted in the inhibition of the differentiation/myelination of oligodendrocytes (10).

The formation and maintenance of the microtubule network dynamics during differentiation, cellular polarization, and migration rely on the pronounced reorganization of the cytoskeleton (11–13). Several factors have been postulated to affect the dynamics of the microtubule system. First, the binding of microtubule-associated proteins (MAPs) to the microtubules increases their stability (14, 15). Second, tubulin is subjected to a number of post-translational modifications, such as phosphorylation, acetylation, tyrosination, polyglycylation, and polyglutamylation (16–18). Notably, the reversible post-translational acetylation of α-tubulin at residue Lys-40 correlates with increased stability of the acetylated microtubules (19–21), suggesting a role in the regulation of the microtubule dynamics (20). However, the role of α-tubulin acetylation in the microtubule stabilization is not well defined and has been recently questioned (22).

The α-tubulin acetylation and deacetylation have been under intense investigation. For instance, the class II HDAC6 (histone deacetylase 6) is a well characterized tubulin deacetylase. HDAC6 is ubiquitously expressed and conserved in a wide range of species (23). HDAC6 is unique among the zinc-depen-

* This work was supported by FP6–2003-LIFESCIHEALTH-I: BioSim and by Hungarian National Scientific Research Fund Grants OTKA T-067963 to (J. Ovádi) and OTKA F-49795 and ELTE CellCom RET (to B. S.).

[1] To whom correspondence should be addressed. Tel.: 36-1-279-3129; Fax: 36-1-466-5465; E-mail: ovadi@enzim.hu.

[2] The abbreviations used are: PD, Parkinson disease; DAPI, 4′,6-diamidino-2-phenylindole; FCS, fetal calf serum; MAP, microtubule-associated protein; PBS, phosphate-buffered saline; SPR, surface plasmon resonance; TSA, trichostatin A; VBL, vinblastine; Dox, doxycycline; siRNA, small interfering RNA; Pipes, 1,4-piperazinediethanesulfonic acid.

dent HDACs in many respects. For instance, HDAC6 has a primary cytoplasmic localization, and its inhibition by a specific inhibitor or by RNA interference can increase the level of acetylated tubulin and alter cell motility (24). SIRT2 (silent information regulator 2) is another tubulin deacetylase implicated in the mitotic regulation of the microtubule dynamics through its binding to HDAC6 (25). SIRT2 is expressed in oligodendrocytes and decelerates cellular differentiation through deacetylation of α-tubulin. The knockdown of SIRT2 in oligodendrocytes increased α-tubulin acetylation and the complexity of cellular arborization, whereas its overexpression had the opposite effect (26). Much less is known about the tubulin acetyltransferase(s) responsible for tubulin acetylation. Very recently, a report has suggested that an acetyltransferase complex consisting of *N*-acetyltransferase 1 and arrest-defective 1 mediates tubulin acetylation (27). Furthermore, a six-subunit histone acetyltransferase elongator complex has been identified in neuronal cells as being responsible for tubulin acetylation (28).

The disturbance of the α-tubulin acetylation level may play a role in the etiology of certain neurodegenerative diseases, such as PD and Huntington disease (29, 30). Notably, the degree of α-tubulin acetylation was found to be low in Huntington disease brains, and the microtubule-dependent transport of vesicles containing the brain-derived neurotrophic factor was reduced, leading to neuronal cell death (30). In striatum-derived neuronal cell lines, the inhibition of HDAC6 by trichostatin A (TSA) increased the amount of acetylated microtubules and stimulated the vesicular transport of the brain-derived neurotrophic factor (30). In models of PD, SIRT2 inhibition was found to rescue α-synuclein-induced neuronal toxicity (29) by causing resistance to axonal degeneration in cerebellar granule neurons (31).

In this work, we studied the effects of TPPP/p25 on the tubulin acetylation and on the organization and dynamics of the microtubule network in three different cell lines showing different expression levels of TPPP/p25. Our results suggest that the expression of TPPP/p25 inhibits HDCA6 activity and promotes acetylation of the microtubule network. Moreover, we provide evidence that the stability of the microtubule network is affected by the bundling activity of TPPP/p25 and not necessarily by the concomitant enhancement of α-tubulin acetylation. We also show that TPPP/p25 affects both the growth velocity of microtubules plus ends and the microtubule-derived cell motility.

EXPERIMENTAL PROCEDURES

Cell Cultures, Transfection, and Manipulations—The HeLa cells (CCL-2) (ATCC) were grown in Dulbecco's modified Eagle's medium supplemented with 10% fetal calf serum (FCS), 1 mM sodium pyruvate, 100 unit/ml streptomycin, and 100 μg/ml penicillin (all reagents from Sigma) in a humidified incubator at 37 °C with 5% CO_2. The cells were grown on 12-mm diameter coverslips for microscopic analysis and on 60-mm dishes for all other experiments. Transfections of HeLa cells with the pEGFP-TPPP/p25 (9), pDsRed2-TPPP/p25, EB3 (pGFP-End-binding protein 3) (kindly provided by Niels Galjart, MGC. Department of Cell Biology and Genetics, Erasmus Medical Center, Rotterdam, The Netherlands), and pEGFP-C1 (Clontech) plasmids were carried out using Fugene HD reagent (Roche Applied Science) according to the manufacturer's instructions. The samples were analyzed 24 h after transfection by immunocytochemistry. When indicated, the cells were treated with TSA (10 nM or 500 nM, overnight) or nocodazole (0.4 μM, 30 min) (all reagents obtained from Sigma). The combined TSA/nocodazole treatment was carried out by treating the samples with nocodazole (0.4 μM, 30 min) before the end of the incubation with TSA (500 nM, overnight). For cold depolymerization, the cells were incubated at 4 °C for 90 min before fixation. For cell motility and EB3 measurements, the cells were treated with either TSA (500 nM) or paclitaxel (40 nM) for 4 h before monitoring.

The CG-4 cells (a kind gift of Dr. Jean-Claude Louis (Amgen)) were propagated in Dulbecco's modified Eagle's medium-N1 medium containing 30% of the same medium conditioned by the neuroblastoma cell line B104 (70/30 medium) (32), 100 units/ml streptomycin, and 100 μg/ml penicillin (all reagents from Sigma). To promote the maturation of oligodendrocyte progenitor cells into differentiated oligodendrocytes, the CG-4 cells were grown in Dulbecco's modified Eagle's medium-N1 supplemented with 40 ng/ml triiodothyronine (Sigma) and 20 ng/ml ciliary neutrophic factor (Sigma) (33). To induce differentiation, the cells were incubated in the differentiation medium for an additional 4 days. For immunofluorescence microscopy, 2×10^4 cells were plated onto poly-L-ornithine-coated glass coverslips and transfected for 24 h with 20 ng of siRNAs using Fugene HD reagent (Roche Applied Science). For immunoblotting, the CG-4 cells were plated onto poly-L-ornithine-coated 6-well plates (10^5 cells/well) and transfected with 120 ng of siRNAs using Fugene HD reagent (Roche Applied Science).

The doxycycline-inducible CHO-K1 Tet-On cell line (provided by Prof. Gyula Hadlaczky, Biological Research Center, Szeged, Hungary) was maintained in Dulbecco's modified Eagle's medium supplemented with 10% Tet-On approved FCS (Clontech) according to the manufacturer's description. The transfection with pTRE2hyg-TPPP/p25 was carried out with Fugene HD reagent (Roche Applied Science) according to the manufacturer's instructions, and a TPPP/p25 stable expressing clone (CHO10) was further selected after subcloning. For Western blot analysis, 2×10^4 CHO10 cells were plated in the standard medium (control) or in the induction medium obtained by adding 50 or 500 nM doxycycline (+Dox) and incubated for 7 days. On day 6, the cells were split and cultured with or without doxycycline (−Dox).

DNA Manipulation—The coding sequence of TPPP/p25 was obtained by PCR using the pEGFP-TPPP/p25 plasmid (9) as template and the primers 5′-AGATACACATATGGCTGACAAGGCTAAGC-3′ and 5′-GTGCTCGAGCTTGCCCCCTTGC-3′. The PCR fragment was digested with XhoI and NdeI and cloned between the appropriate restriction sites of the pET21c vector (Novagen), resulting in the pET21c-TPPP/p25 plasmid. For the construction of the pDsRed2-p25 plasmid, the same template was amplified using the following primers: 5′-AGATACTCGAGGGATGGCTGACAAGGCTAAGC-3′ and 5-ATCGAATTCCTACTTGCCCCCTTGCACCTTCTGG-3′. The PCR product was digested with XhoI and EcoRI and

ligated in the pDsRed2-C1 vector (Clontech). For the pTRE2hyg-TPPP/p25 construct, the same template was used with the primers 5′-AGATAGGATCCGGATGGCTGACAAGGCTAAGC-3′ and 5-ATCGCTTAGCTACTTGCCCCCTTGCACCTTCTGG-3′. After digestion with BamHI and NheI, the insert was ligated in the pTRE2hyg vector (Clontech). All constructs were verified by DNA sequencing.

siRNA Experiments—The siRNA1 (5′-CCAAUCAGGAAAGGGCAAGGGCAAA-3′) against TPPP/p25 was obtained from Invitrogen. A fluorescently labeled scrambled siRNA (Santa Cruz Biotechnology, Inc. (Santa Cruz, CA)) was used as a negative control.

Protein Purification—Recombinant human TPPP/p25 was expressed in *Escherichia coli* BL21 (DE3) cells and isolated on HIS-Select™ cartridge (catalog no. H8286, Sigma) as described previously (8).

Differential Extraction of Tubulin Species—The differential extraction of tubulin and microtubules from the cellular samples was performed using a two-step extraction procedure (34). In brief, 10^5 HeLa cells/well were plated in a 6-well tissue culture plate and incubated overnight. The cells were treated with the agents 500 nM TSA for 4 h and 40 nM paclitaxel or 500 nM vinblastine (VBL) for 1 h, and the combined TSA/VBL treatment was carried out by adding 500 nM VBL for 1 h before the end of the TSA treatment. At the end of the incubation, the cells were washed with prewarmed phosphate-buffered saline (PBS), and the soluble tubulin fraction was isolated *in situ* by using 100 μl of microtubule-stabilizing buffer (80 mM Pipes) (pH 6.8), 1 mM $MgCl_2$, 1 mM EGTA, 0.5% Triton X-100, 10% glycerol and protease inhibitors) (all from Sigma) prewarmed at 37 °C and by keeping the tissue culture plate at the same temperature. Next, the cells were quickly washed with prewarmed microtubule-stabilizing buffer, and the fractions of polymerized microtubules were extracted in 100 μl of microtubule-destabilizing buffer (20 mM Tris (pH 7.4), 150 mM NaCl, 1% Triton X-100, 10 mM $CaCl_2$, and protease inhibitors) (all from Sigma) at room temperature. The extracts were chilled on ice, and both fractions were centrifuged to obtain a clarified supernatant for SDS-PAGE.

Immunoblotting—For Western blot analysis, the cells were lysed in 100 μl of radioimmune precipitation buffer supplemented with protease inhibitors (both obtained from Sigma). After lysis, the samples were centrifuged, and supernatants were kept at −70 °C. The tubulin, acetylated tubulin, and TPPP/p25 were detected by using a monoclonal antibody against α-tubulin (DM1A, Sigma), Lys-40-acetylated-α-tubulin (6-11B-1, Sigma) and rat polyclonal sera against recombinant TPPP/p25 (5), respectively.

Immunocytochemistry—For immunofluorescence microscopy analysis, the HeLa cells were fixed with ice-cold methanol for 10 min. After 15 min in PBS, the samples were blocked for 30 min in PBS containing 0.1% Triton X-100 (TPB) and 5% FCS (TPB-FCS). The cells were stained with a monoclonal α-tubulin antibody (1:1000, DM1A, Sigma) or a monoclonal antibody against Lys-40-acetylated-α-tubulin (1:1000, 6-11B-1, Sigma), followed by Texas Red-conjugated anti-mouse antibody (1:1000, Invitrogen). The samples were washed for 7 min, three times with TPB after each antibody incubation.

The CG-4 cells were fixed for 5 min using 0.25% glutaraldehyde (EM grade, Sigma) and 4% paraformaldehyde (Sigma). The cells were rinsed in PBS (three times for 5 min each), and residual glutaraldehyde was quenched by 0.1 M NH_4Cl. The samples were blocked in TPB-FCS for 30 min and sequentially incubated for 2 h in the presence of the primary and secondary antibodies. The rat polyclonal serum against recombinant TPPP/p25 (5) and the monoclonal antibody against Lys-40-acetylated-α-tubulin were used as described above. The affinity-purified secondary antibodies against mouse and rat IgGs conjugated with Texas Red or Alexa-488 were obtained from Invitrogen.

The coverslips were mounted with GelMount (or Crystal-Mount) and sealed with Clarion (all reagents from Biomeda). Nuclei were counterstained with 4,6-diamidino-2-phenylindole (DAPI).

Microscopy—The pictures of fixed samples were acquired on a Leica DMLS epifluorescent microscope as described previously (9). For densitometric analysis, the images were collected under constant exposure parameters. The determination of acetylated tubulin or TPPP/p25 levels was performed by using the Analyze, Measure option of the National Institutes of Health ImageJ software. The whole territory of each cell was outlined by the Freehand Line tool and analyzed by taking the sum of the gray values of the pixels in the selection (integrated density (IntDen)) and by subtracting the background.

The time lapse recordings were performed on a computer-controlled Leica DM IRB inverted microscope equipped with ×20/0.4 N-Plan (for cell motility) or ×100 (for EB3-GFP motility). The cell cultures were kept at 37 °C in a humidified 5% CO_2 atmosphere within a CellMovie incubator attached to the microscope. The objective ×100/1.2–0.6 W N-Plan was equipped with an objective heating ring for temperature control. The fluorescent images were acquired every 10 min for 3 days to follow the cell motility or every 5 s for 2 min to determine the GFP-EB3 motility. All images and videos were processed using the ImageJ software, and data were analyzed using the Microsoft Excel software. For time lapse experiments, the Particle Analysis, Manual Tracking plug-in of ImageJ was used. For cell motility analysis, the position of the cells in each time lapse frame was determined by taking the center of the nuclei. For the measurement of GFP-EB3 motility, the tip of the GFP-EB3 dashes was determined for every frame. Only dashes that could be followed for at least three consecutive frames were taken into account.

Surface Plasmon Resonance (SPR)—SPR measurements were performed on a BIAcore X instrument (GE Healthcare). A stock solution of HDAC6 (0.6 mg/ml) was diluted into 50 mM sodium acetate (pH 4.0) at a final concentration of 10 μg/ml. 100 μl of this solution was then injected at a flow rate of 5 μl/min on a CM5 sensorchip activated by the amine coupling method according to the manufacturer's instructions. The control flow cells were prepared similarly except that the coupling assay did not contain HDAC6. For the measurements of the interaction between HDAC6 with TPPP/p25, 30–60 μl of TPPP/p25 samples were injected at different concentrations over the HDAC6-covered surface at a flow rate of 10 μl/min. To characterize the interaction of HDAC6 with the TPPP/p25-tubulin complex, a

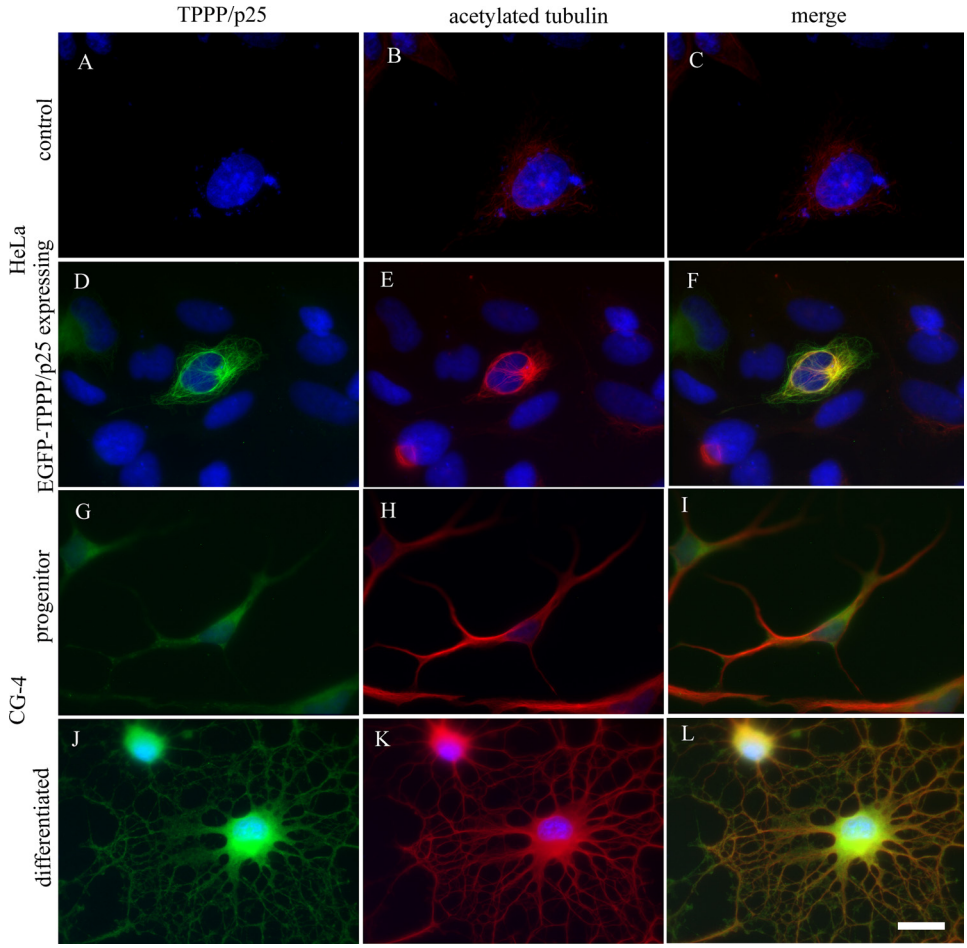

FIGURE 1. **Increased tubulin acetylation in TPPP/p25-expressing cells.** Immunostaining for TPPP/p25 (*green*) and acetylated tubulin (*red*) in untransfected (*A–C*) and pEGFP-TPPP/p25-transfected (*D–F*) HeLa cells and in oligodendrocyte progenitor (*G–I*) and differentiated (*J–L*) CG-4 cells. HeLa cells virtually did not have endogenous TPPP/p25 (*A*). TPPP/p25 was detected only after transfection (*D*). The level of acetylated tubulin was very low in HeLa cells (*B*). However, it increased in TPPP/p25-expressing cells (*E*). The oligodendrocyte progenitor CG-4 cells expressed endogenous TPPP/p25 (*G*), and the tubulin was acetylated (*H*). In differentiated oligodendrocytes, TPPP/p25 (*J*) and acetylated tubulin (*K*) levels were higher when compared with that of the progenitor cells. *Blue*, DAPI. *Scale bar*, 10 μm.

constant concentration of TPPP/p25 (90 nM) complexed with different concentrations of tubulin was injected under the same condition. The binding and dissociation of TPPP/p25 and the TPPP/p25-tubulin complex were performed in 10 mM 4-(2-hydroxyethyl)-1-piperazineethanesulfonic acid (pH 7.4) buffer containing 150 mM NaCl and 0.005% P-20 detergent (GE Healthcare). After each cycle, the chips were regenerated by injecting 50 mM NaOH for 30 s. All experiments were repeated at least three times. The steady-state binding level of TPPP/p25 to HDAC6 was evaluated by non-linear fitting using the BIAEvaluation 4.1 software.

HDAC6 Activity Assay—HDAC6 activity was measured using a fluorimetric HDAC6 assay kit (BPS Bioscience, San Diego, CA) according to the manufacturer's protocol. The half-maximal (50%) inhibitory concentration of TPPP/p25 (IC_{50}) was determined from the relative inhibitory effect *versus* TPPP/p25 concentration plot.

Statistical Analysis—The *error bars* represent the S.E. Comparisons were performed using Student's *t* test, and values were considered to be significant if the calculated *p* value was <0.05 (shown by an asterisk).

RESULTS

TPPP/p25 Promotes Tubulin Acetylation—Our preliminary data indicated that the microtubule network of HeLa cells was acetylated following TPPP/p25 transfection. To further characterize the relationship between TPPP/p25 expression and tubulin acetylation, we used three cell lines showing different expression levels of TPPP/p25. The HeLa cells did not express TPPP/p25 endogenously, as revealed by immunocytochemistry using a specific TPPP/p25 antibody (Fig. 1*A*). However, TPPP/p25 was aligned along the microtubule network when the cells were transfected with the pEGFP-TPPP/p25 plasmid (Fig. 1*D*). In both oligodendrocyte CG-4 progenitor cells (Fig. 1*G*) and differentiated CG-4 cells (Fig. 1*J*), TPPP/p25 was expressed endogenously, with levels consistent with a strong up-regulation of TPPP/p25 during oligodendrocyte differentiation (10).

To visualize the level of α-tubulin acetylation together with TPPP/p25 expression, the cells were immunostained with a monoclonal antibody against acetylated Lys-40 of α-tubulin. The level of acetylated tubulin was rather low in HeLa cells (Fig. 1*B*). However, its expression was remarkably promoted by TPPP/p25 (Fig. 1*E*). In contrast to HeLa cells, the CG-4 progenitor cells, which expressed TPPP/p25 endogenously, showed immunopositivity for acetylated tubulin (Fig. 1*H*). The level of tubulin acetylation increased concomitantly with that of TPPP/p25 during the differentiation of oligodendrocytes (Fig. 1*K*), in agreement with a necessary role of tubulin acetylation during cellular maturation (26, 28).

To establish the role of TPPP/p25 in tubulin acetylation, TPPP/p25 was down-regulated by using previously validated siRNA (10). Notably, the down-regulation of TPPP/p25 by siRNA1 (Fig. 2*C*) in CG-4 progenitor cells led to a decreased acetylated tubulin level (Fig. 2*A*) when compared with the untransfected cells (Fig. 2, *D* and *B*; respectively). We quantified this effect by measuring the fluorescence signals of individual cells after immunostaining of the samples with TPPP/p25 and acetylated tubulin antibodies (Fig. 2*E*). These data showed a 40% decrease in TPPP/p25 level and an ~20% decrease in acetylated tubulin level. This finding was further confirmed by Western blot analysis of the progenitor cells transfected with siRNA1 (Fig. 2*F*), where concomitant reduction of TPPP/p25 and acetylated tubulin levels was also

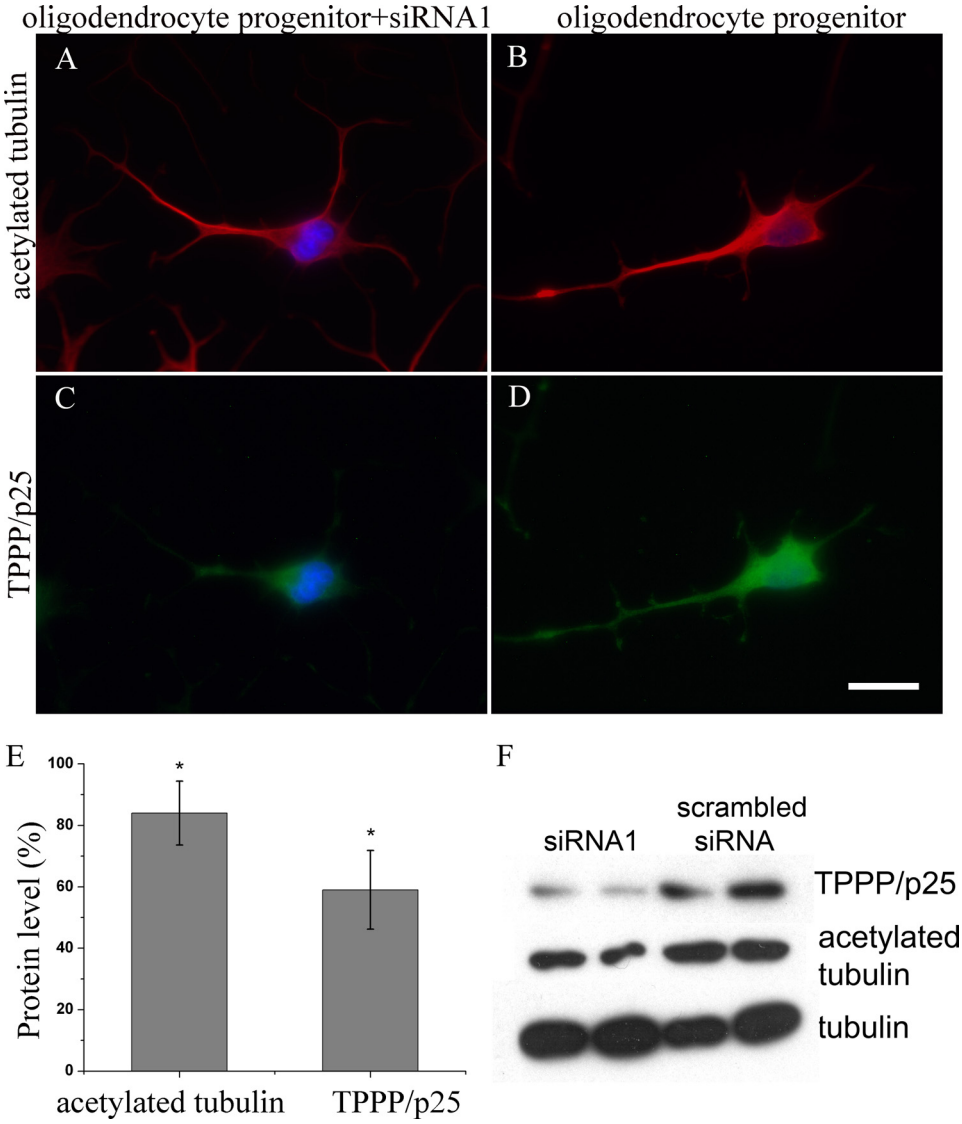

FIGURE 2. **Decreased tubulin acetylation in TPPP/p25-depleted CG-4 progenitor cells.** CG-4 progenitor cells were immunostained for acetylated tubulin (*A* and *B*, *red*) and for TPPP/p25 (*C* and *D*, *green*). Down-regulation of TPPP/p25 by siRNA1 resulted in a decrease of both TPPP/p25 (*D versus C*) and acetylated tubulin levels (*B versus A*). *Blue*, DAPI. *Scale bar*, 10 μm. Acetylated tubulin and TPPP/p25 levels were quantified by the fluorescence signal of individual cells, as described under "Experimental Procedures," and were expressed relative to the protein levels measured in the control, untransfected cells (100%) (*E*). *Error bars*, S.E., $n = 100$. *, significant difference in the level of acetylated tubulin and TPPP/p25 between control and transfected samples (according to Student's *t* test, $p < 0.05$). Western blot analysis of acetylated tubulin and TPPP/p25 levels after transfection of CG-4 progenitor cells with siRNA1 (*F*, *lanes 1* and *2*, from parallel samples) and with scrambled siRNA (*F*, *lanes 3* and *4*, from parallel samples). Tubulin was used as a loading control. A representative result of three separate experiments is shown.

detected when compared with the control sample transfected with a scrambled siRNA.

To further explore the influence of TPPP/p25 on tubulin acetylation, we used a stable TPPP/p25-expressing CHO-K1 Tet-On cell line denoted CHO10. The uninduced CHO10 cells (no doxycycline) showed a basal activity of the promoter (leakage), generating a low level of TPPP/p25 (control). When the cells were incubated with 50 or 500 nM doxycycline (Dox 50 or Dox 500, respectively), TPPP/p25 was expressed extensively, which resulted in the enhancement of tubulin acetylation, as revealed by immunoblotting (Fig. 3*A*). The total tubulin of each sample was found to be virtually constant and was used to normalize the relative changes of TPPP/p25 and tubulin acetylation (Fig. 3*B*). The extent of TPPP/p25 expression was dependent on the doxycycline concentration. Notably, a higher TPPP/p25 expression level caused more pronounced acetylation of the microtubules. The subsequent withdrawal of the doxycycline (−Dox 50, −Dox 500) from the medium extensively decreased the level of TPPP/p25, and this was coupled with a slight reduction in tubulin acetylation. This observation is consistent with what was observed with the CG-4 progenitor cells, where a 40% decrease in the level of TPPP/p25 after siRNA1 transfection caused less than 20% reduction in the tubulin acetylation level. Of note, the production of a similar amount of TPPP/p25 level with 50 nM doxycycline or after withdrawal of 500 nM doxycycline resulted in a similar acetylated tubulin level, confirming that TPPP/p25 is a modulator of tubulin acetylation.

TPPP/p25 Promotes Tubulin Acetylation by Inhibiting HDAC6-mediated Deacetylation—To evaluate the contribution of acetylation-related enzyme to the acetylation level of tubulin in relation to TPPP/p25 expression, we modulated the level of tubulin acetylation using TSA as an inhibitor of HDAC6.

The changes in tubulin acetylation level were quantified by measuring the fluorescence signals of individual cells after immunocytochemistry for acetylated tubulin in HeLa cells expressing EGFP-TPPP/p25 and in control (untransfected) cells (Table 1). Our results showed that the presence of TPPP/p25 increased α-tubulin acetylation by 70% when compared with the untransfected cells (control cells = 100%). The TSA treatment (at 10 and 500 nM) resulted in higher acetylation level (256 and 487%, respectively) when compared with control. The addition of 10 nM TSA to the TPPP/p25-expressing cells increased further the TPPP/p25-derived tubulin acetylation (534%), whereas a higher concentration of TSA (500 nM) did not raise further the acetylation level (490%), indicating that all Lys-40 residues of the microtubule network became post-translationally modified at this inhibitor concentration and that all of the available Lys-40 residue-related epitopes were occupied by acetylated tubulin antibodies. These findings suggest that the promoting effect of TPPP/p25 on tubulin acetylation could result either from the

inhibition of the deacetylase activity of HDAC6 or from the activation of the tubulin acetyltransferases.

To address this hypothesis, we performed *in vitro* binding experiments with TPPP/p25 and HDAC6 as well as functional studies to establish the inhibitory effect of TPPP/p25 on HDAC6 activity. As previously shown, *S*PR is an appropriate method to characterize the binding of TPPP/p25 to its potential targets, such as tubulin (35, 36); thus, the binding of TPPP/p25 to HDAC6 was demonstrated by SPR measurements. HDAC6 was covalently immobilized on the chip, and different concentrations of TPPP/p25-containing solutions were injected over the surface. A typical sensorgram measured at 200 nM TPPP/p25 is shown in Fig. 4*A* with the fitted curve used to obtain the steady-state (equilibrium) value of bound TPPP/p25 (in response units (*RU*)). The steady-state values were plotted as a function of TPPP/p25 concentration to evaluate the apparent dissociation constant (K_d) of the heteroassociation of HDAC6 with TPPP/p25 (Fig. 4*B*), which was found to be 112 ± 20 nM.

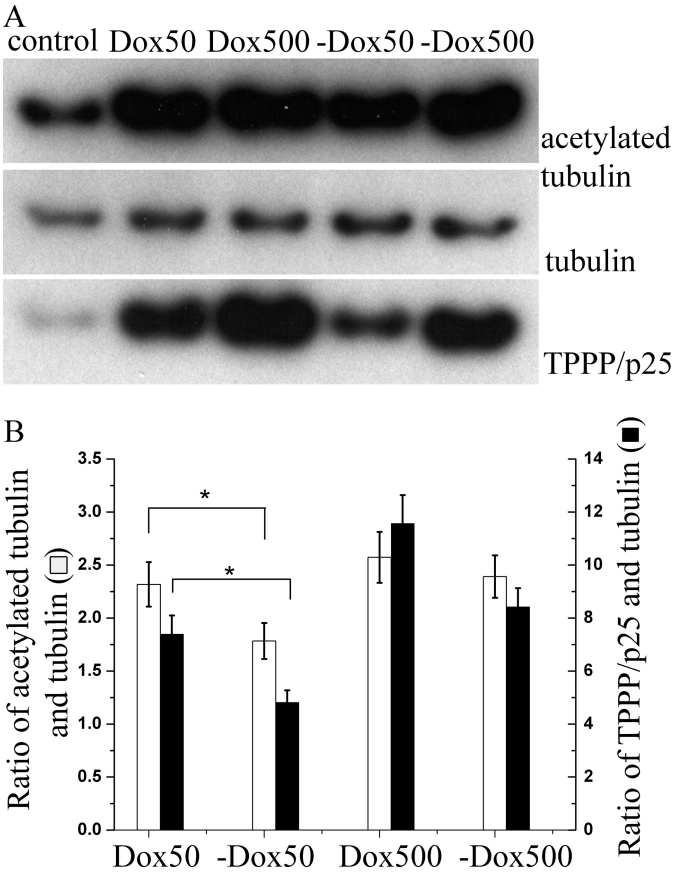

FIGURE 3. **Level of TPPP/p25 modulates the level of acetylated tubulin in the doxycycline-inducible CHO10 cell line.** Western blot analysis of TPPP/p25, α-tubulin, and acetylated tubulin in the CHO10 cell line after doxycycline induction (*A*). Quantification of proteins by densitometry showed that 50 or 500 nM doxycycline (*Dox 50* or *Dox 500*) induced a robust increase of the TPPP/p25 level with a concomitant increase of the acetylated tubulin level, whereas withdrawal of doxycycline (*−Dox 50*, *−Dox 500*) resulted in a drop of both proteins. As a control, the level of α-tubulin remained constant among the samples (*B*). TPPP/p25 and acetylated tubulin values were normalized after dividing these values by the corresponding control and tubulin values. *Error bars*, S.E. *, significant difference in the ratio of acetylated tubulin and tubulin and in the ratio of TPPP/p25 and tubulin between the Dox 50 and −Dox 50 samples, respectively {according to Student's *t* test, $p < 0.05$}. Results are the average of three independent experiments.

To establish whether tubulin counteracts the binding of TPPP/p25 to HDAC6, 90 nM TPPP/p25 mixed with different concentrations of tubulin was injected over the surface covered with HDAC6. As illustrated in Fig. 4*B*, the increase of tubulin concentration reduced the amount of TPPP/p25 bound to the immobilized HDAC6. At 1 μM tubulin concentration, the sensorgram indicated no protein binding to the HDAC6 immobilized on the chip. A plausible explanation for this finding is that TPPP/p25 complexed with tubulin does not associate with HDAC6.

The functional effect of TPPP/p25 binding on HDAC6 activity was measured using a fluorometric HDAC6 assay. The addition of TPPP/p25 to the HDAC6 assay resulted in a concentration-dependent inhibition, reaching almost full (90%) inhibition of HDAC6 activity *in vitro*. The IC_{50} value evaluated from the dose-response curve was 350 ± 60 nM (Fig. 4*C*).

Effects of TPPP/p25 and Tubulin Acetylation on the Stabilization of the Microtubule Network—We previously showed that TPPP/p25 expression causes microtubule resistance to the anti-microtubular agent VBL and suggested a role of the TPPP/p25 bundling activity in microtubule stabilization (9). We sought to determine whether this TPPP/p25-derived bundling activity and/or the TPPP/p25-derived tubulin acetylation was responsible for the stabilization of the microtubules.

In a first set of experiments, the microtubule stability of HeLa cells transiently transfected with the pEGFP-TPPP/p25 plasmid was investigated by fluorescence microscopy in the absence or in the presence of the anti-microtubular agent nocodazole (Fig. 5) or by incubating the cells at low temperature. The α-tubulin immunostaining showed that the organization of the microtubule network in untransfected cells (control

TABLE 1

Effect of TPPP/p25 on the acetylation level of microtubules modulated by the inhibitor of HDAC6

HeLa cells transiently transfected with the pEGFP-TPPP/p25 were treated with 10 nM or 500 nM TSA (HDAC6 inhibitor). After overnight incubation, the cells were immunostained for acetylated tubulin. The fluorescence signal of individual cells was quantified to obtain the acetylation level and expressed relative to the degree of acetylation observed for control cells (100%). The status of the microtubules (normal, bundled, or depolymerized) was also determined. Values are shown ± S.E. *n* (control) = 63, *n* (10 nM TSA) = 121, *n* (500 nM TSA) = 36, *n* (TPPP/p25) = 43, *n* (TPPP/p25 + 500 nM TSA) = 21, *n* (TPPP/p25 + 10 nM TSA) = 39. These data are representative of three independent experiments.

	Acetylation level	Microtubules	Cold/nocodazole treatment	Cold/nocodazole treatment after TSA treatment
	%			
Control	100 ± 12	Normal	Depolymerized	Depolymerized
10 nM TSA	256 ± 9[a]	Normal	Depolymerized	Depolymerized
500 nM TSA	487 ± 16[a]	Normal	Depolymerized	Depolymerized
TPPP/p25	170 ± 15[a]	Bundled	Bundled	Bundled
TPPP/p25 + 10 nM TSA	534 ± 16[a]	Bundled	Bundled	Bundled
TPPP/p25 + 500 nM TSA	490 ± 21[a]	Bundled	Bundled	Bundled

[a] Significant difference in the level of acetylated tubulin between drug treated/transfected cells and control cells (according to Student's *t* test, $p < 0.05$).

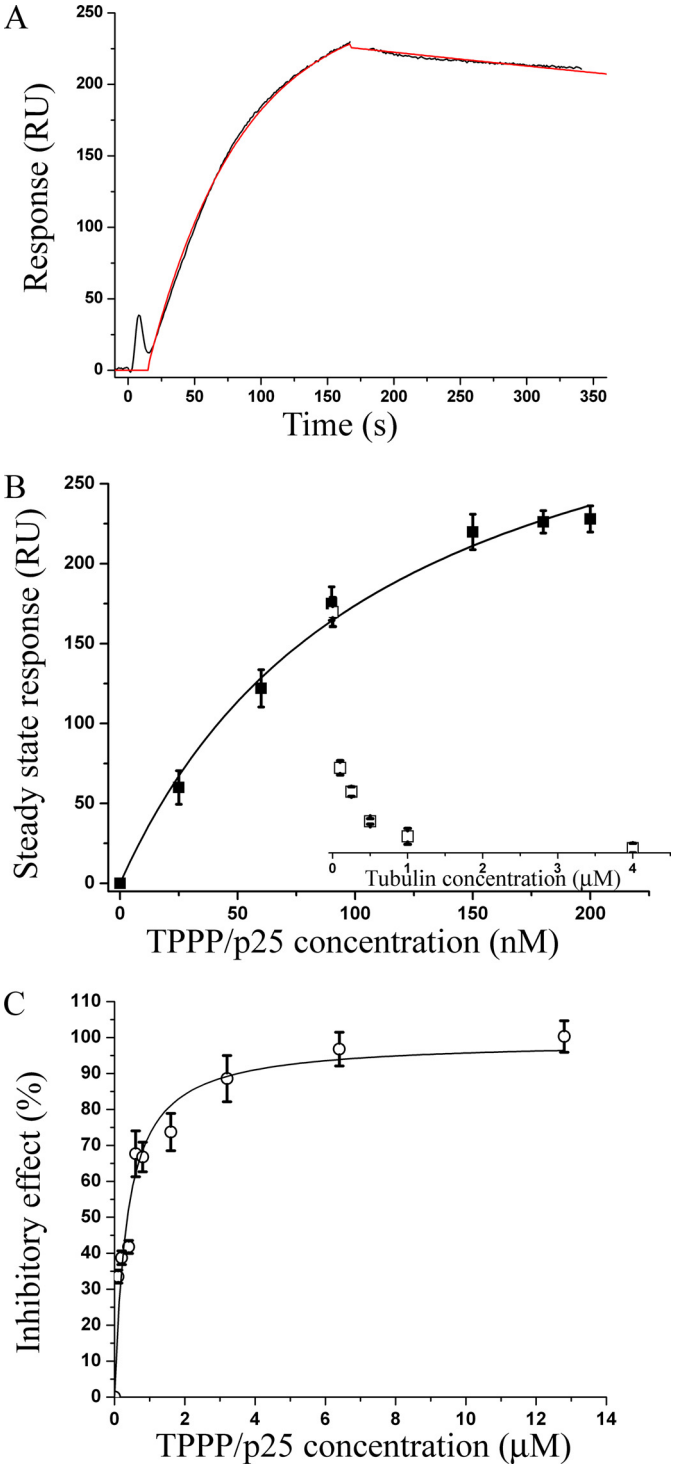

FIGURE 4. **Interaction of TPPP/p25 with HDAC6 and its effect on the deacetylase activity.** Binding of TPPP/p25 to immobilized HDAC6 was detected by SPR measurements. A typical sensorgram was recorded after injecting 200 nM TPPP/p25 onto the chip for 3 min, followed by the loading buffer to initiate the dissociation of TPPP/p25 from the immobilized HDAC6 (*black*). The sensorgram was fitted to determine the steady-state value (*red*) (*A*). Steady-state values of the binding *versus* injected TPPP/p25 concentration showed hyperbolic saturation with an apparent K_d value of 112 ± 20 nM (*B*, ■). The sensorgrams were also recorded when tubulin was present at various concentrations in the injected TPPP/p25 solution (90 nM). The steady-state (equilibrium) values of bound TPPP/p25 were evaluated and plotted as a function of tubulin concentration (*B*, □). Results are the average of three independent experiments. *Error bars*, S.E. The inhibitory effect of TPPP/p25 on the deacetylase activity of HDAC6 was determined by using a commercial fluorimetric enzymatic assay. The IC_{50} value determined from the relative inhibitory effect of TPPP/p25 *versus* TPPP/p25 concentration plot is 350 ± 60 nM (*C*). Results are the average of three independent experiments. *Error bars*, S.E.

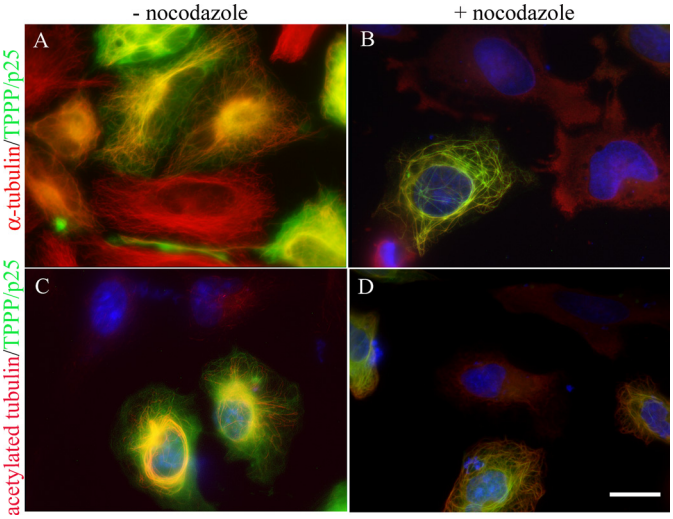

FIGURE 5. **Increased stability of the TPPP/p25 bundled microtubules.** Transiently transfected HeLa cells expressing EGFP-TPPP/p25 (*A–D*, *green*) were immunostained for α-tubulin (*A* and *B*, *red*) and acetylated tubulin (*C* and *D*, *red*) before (*A* and *C*) and after (*B* and *D*) nocodazole treatment. The microtubules of untransfected cells (TPPP/p25-negative cells) were depolymerized after nocodazole treatment, whereas TPPP/p25 bundled microtubules were preserved in the transfected cells (*B* and *D*). The signal for α-tubulin and acetylated tubulin was distributed homogeneously in the cytoplasm (*B* and *D*, untransfected cells). *Blue*, DAPI. *Scale bar*, 10 μm.

cells) appeared as fine filaments radiating from the centrosome toward the periphery, whereas the microtubules were bundled and displayed distinct ultrastructures in the TPPP/p25-expressing cells (Fig. 5*A*). These ultrastructures and the cellular morphology were highly dependent on the expression level of TPPP/p25 (9). The nocodazole treatment of the control cells resulted in the homogeneous distribution of α-tubulin, due to the depolymerization of the microtubules (Fig. 5*B*). In contrast, the bundled microtubules of the TPPP/p25-expressing cells showed resistance to nocodazole, whereas the unbundled microtubules became depolymerized. Similar results were obtained when the disassembly of the microtubules were induced by cold treatment (data not shown). Next, the cells were immunostained for acetylated α-tubulin to visualize the stability of the post-translationally modified microtubule network. A representative fluorescent picture demonstrates that α-tubulin acetylation in HeLa cells was taking place exclusively in TPPP/p25-expressing cells (Fig. 5*C*) that were showing resistance to nocodazole (Fig. 5*D*) and cold treatment (data not shown) in case of bundling.

To monitor the effect of acetylation on the microtubule network, a similar set of experiments was performed; however, the cells were also treated with TSA. Due to the inhibition of HDAC6, virtually all of the microtubules became acetylated (Fig. 6*A*). The microtubule network was similar to that of the untreated cells immunostained for α-tubulin (Fig. 5*A*). In addition, the microtubule network of TPPP/p25-expressing cells was also bundled (Fig. 6*A*), suggesting that the bundling effect apparently was not affected by the acetylation status of the

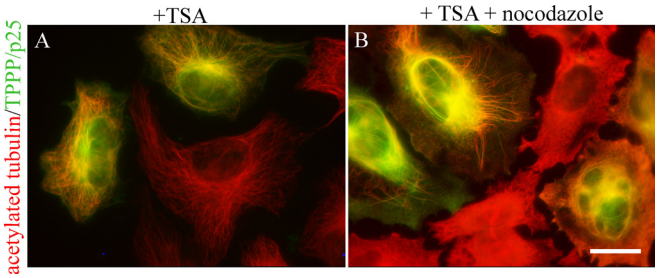

FIGURE 6. **Microtubule stabilization by TPPP/p25 is acetylation independent.** HeLa cells were transiently transfected with the pEGFP-TPPP/p25 plasmid (*green*) and treated with TSA (*A*) or with nocodazole before the end of the overnight TSA treatment (*B*) and immunostained for acetylated tubulin (*red*). Note that 500 nM TSA significantly increased the level of acetylated tubulin (*A*). Remarkably, the subsequent nocodazole treatment caused depolymerization of the microtubule network only in non-transfected cells (*B*, *red only*) whereas the TPPP/p25 bundled microtubule network was resistant to depolymerization (*B*, *orange*). *Scale bar*, 10 μm.

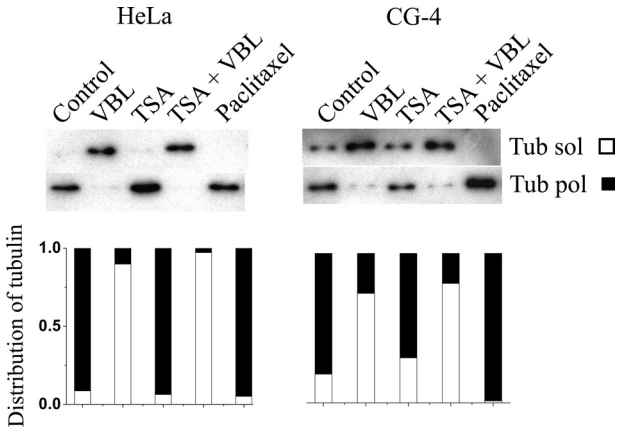

FIGURE 7. **Distribution of tubulin and acetylated tubulin between soluble and polymerized fractions of treated HeLa and CG-4 cells.** Cells were treated with VBL, TSA, TSA plus VBL, or paclitaxel. The soluble (*sol*) and polymerized (*pol*) tubulins were visualized by Western blot using anti-tubulin antibody and quantified by densitometry. The distribution of tubulin between the soluble (*empty bar*) and polymerized (*black bar*) fractions is illustrated by a *stacked bar chart*. For each sample, the total amount of tubulin was calculated by summing the values of the corresponding soluble and polymerized pools. The relative fractions were calculated by dividing the value of each pool by the total amount of tubulin. A representative result of three separate experiments is shown.

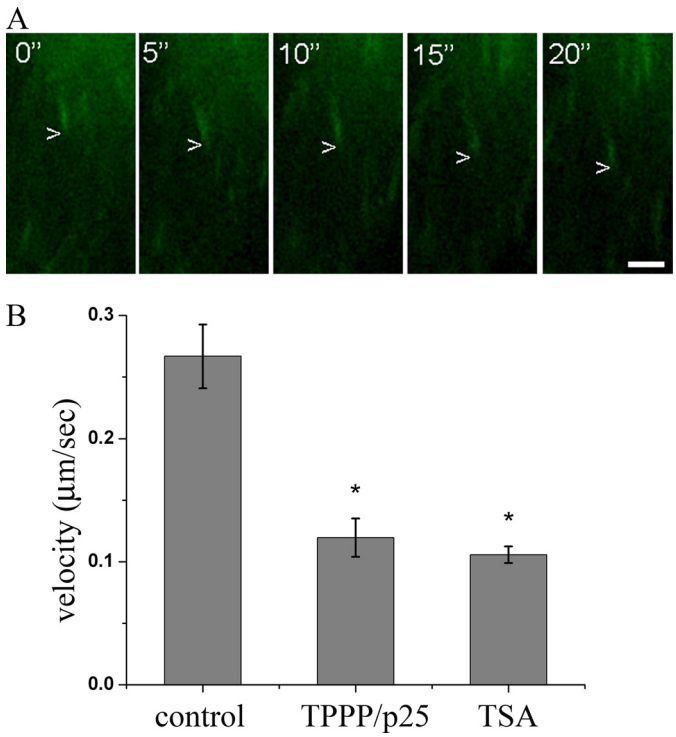

FIGURE 8. **TPPP/p25 decreases microtubule growth velocity.** Shown is the overlap of four successive time lapse images of EB3-GFP taken at 5-s intervals representing the displacement of EB3-GFP as a moving comet tail in a control HeLa cell. *Scale bar*, 2 μm (*A*). The microtubule growth velocity of the DsRed2-TPPP/p25-expressing cells and TSA-treated cells decreased when compared with control cells. The TPPP/p25-decorated or TSA-treated microtubules grew about 2 times more slowly than the microtubules of the control cells (*B*). The *error bars* represent S.E. n (control) = 6, n (TPPP/p25) = 10, n (TSA) = 17. *, significant difference between TSA-treated or TPPP/p25-expressing cells and control cells (according to Student's t test, $p < 0.05$).

microtubule network. The subsequent addition of TSA and nocodazole resulted in a complete depolymerization of the acetylated microtubules in the untransfected cells. In contrast, within the TPPP/p25-expressing cells, only the unbundled microtubules became depolymerized, whereas the bundled microtubules were preserved (Fig. 6*B*). A similar effect was observed after cold treatment (data not shown), further suggesting that TPPP/p25 induces microtubule stabilization via its microtubule bundling activity and independently of its concomitant acetylation-promoting activity.

In another set of experiments, the stability of the microtubule network of HeLa cells and CG-4 progenitor cells was assessed in the absence and presence of paclitaxel, TSA, VBL, or TSA plus VBL. The partition of the soluble and polymerized tubulins was quantified by immunoblotting using an α-tubulin antibody (Fig. 7). In untreated HeLa cells, the tubulin appeared predominantly in a polymerized form, whereas it was distributed between the two fractions in CG-4 progenitor cells. After VBL treatment, the partition of the tubulin between the two fractions was altered; mainly all tubulin appeared in the soluble fraction in both cell types. In the presence of paclitaxel, as expected, the polymerized form of tubulin was exclusively detected. Because the acetylation of the microtubules produced by TSA treatment virtually did not protect microtubules from the depolymerization induced by VBL (TSA plus VBL), this indicates that tubulin acetylation did not increase the stability of the microtubules (Fig. 6). Of note, the expression level of the endogenous TPPP/p25 was rather low in CG-4 progenitor cells; thus, its effect on microtubule stabilization was slight. However, a small amount of polymerized tubulin could be detected in the presence of VBL, whereas in HeLa cells, which did not express endogenous TPPP/p25, the depolymerization was complete.

Effect of TPPP/p25 on the Dynamics of the Microtubule System—The inhibition of HDAC6 has been proposed to regulate the dynamics of the microtubule network (37). Because we identified TPPP/p25 as a novel inhibitor of HDAC6, we thought to establish the effects of TPPP/p25 on the dynamics of the microtubule system.

We examined the growth velocity of the microtubules by time-lapse video microscopy using the GFP-coupled plus-end-tracking protein EB3 as a powerful marker to visualize microtubule dynamic events (38). As shown in Fig. 8*A*, the GFP-EB3 protein appeared as many moving fluorescent dashes at the tip of the microtubules. The growth velocity was calculated by

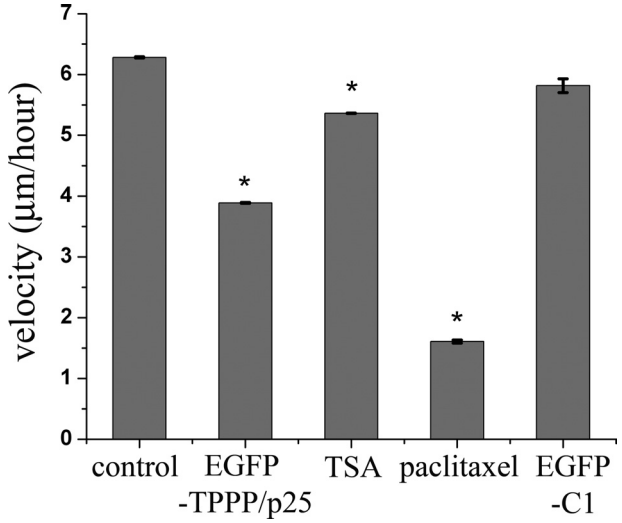

FIGURE 9. **TPPP/p25 expression decreases cell motility.** The effect of TPPP/p25 expression on cell motility was monitored by time lapse video microscopy. The quantification of the velocity showed that both TPPP/p25-expressing cells and TSA-treated cells (500 nM) moved more slowly than control cells. The expression of EGFP alone (after transfection with the pEGFP-C1 plasmid) had no influence on the velocity of the cells. The incubation with paclitaxel (40 nM) gave the highest motility retraction. *Error bars*, S.E. n (control) = 110, n (paclitaxel) = 9, n (EGFP-C1) = 10, n (TPPP/p25) = 52, n (TSA) = 86. *, significant difference between drug-treated or transfected and control cells (according to Student's t test, $p < 0.05$). A representative result of three separate experiments is shown.

superimposing two successive images taken at 5-s intervals and by measuring the velocity of the displacement of the microtubule tips. In this experiment, the HeLa cells were transiently transfected with the pDsRed-TPPP/p25 construct, which rendered it possible to monitor GFP-EB3 in parallel. Treatment of HeLa cells with TSA significantly decreased the degree of the tip displacement and hence the microtubule growth velocity (Fig. 8*B*), consistent with a previous observation obtained with melanoma cells (37). The analysis of the microtubule growth velocities in the TPPP/p25-expressing cells revealed that the presence of TPPP/p25 produces a reduction in the growth velocity, similar to that observed after TSA treatment (Fig. 8*B*). Therefore, it is likely that the growth of the microtubules is affected by the inhibitory effect of TPPP/p25 on HDAC6. This observation underlines that TPPP/p25 acts as a HDAC6 inhibitor and regulates the growth velocity by inhibiting HDAC6, similarly to what has been shown for other HDAC6 inhibitors (37).

We also examined the influence of TPPP/p25 on the cell motility because it was reported that the inhibition of tubulin deacetylation decreased cell motility (12, 39). The changes in cell motility were assayed by measuring velocity of cellular movements by time-lapse microscopy on the basis of their displacement between two successive image frames taken at 10-min intervals. The effect of microtubule acetylation on cell motility was studied on TSA-treated cells, which showed decreased cell motility when compared with untreated cells (Fig. 9). The treatment of these cells with paclitaxel, which stabilizes the microtubules without changing the level of acetylation at the given concentration (40 nM) (20), also decreased cell motility (Fig. 9). The velocity of the EGFP-TPPP/p25-expressing cells was slower and faster when compared with that of TSA- and paclitaxel-treated cells, respectively, whereas the expression of EGFP alone had no influence on cell motility (Fig. 9). Taken together, these results indicate that the expression of TPPP/p25 influences cell motility; however, the precise mechanism of its action requires further investigations because TPPP/p25 regulates both microtubule acetylation and stability, which are two distinct processes regulating cell motility.

DISCUSSION

We previously showed that TPPP/p25 specifically colocalized with the microtubule network of the cytoskeleton in mammalian cell lines and that this colocalization was dynamic (9). We now show that TPPP/p25, in addition to its bundling activity causing microtubule stabilization, promoted acetylation of α-tubulin at Lys-40 along the microtubule network. Our data revealed that the level of tubulin acetylation increased by the expression of TPPP/p25 in HeLa cells and in CHO10 cells (*cf.* Figs. 1 and 3). A similar phenomenon was also observed with the oligodendrocyte-like CG-4 cell line (*cf.* Fig. 1), where increases of TPPP/p25 and acetylated tubulin levels take place in parallel during the differentiation process of the oligodendrocyte progenitor cells into mature oligodendrocytes, whereas down-regulation of TPPP/p25 by specific siRNA results in a simultaneous decrease of TPPP/p25 and acetylated tubulin levels, similar to that observed with the CHO10 cells, where abolition of TPPP/p25 induction caused reduction in the level of the two proteins.

Some contradictory data have been published in the literature concerning the role of tubulin acetylation in the microtubule stabilization (19, 20, 22, 40). Our present data obtained with HeLa cells treated with TSA showed that acetylation itself does not produce stable microtubules, as evidenced by a high sensitivity to the different anti-microtubular treatments, including nocodazole and cold exposure (*cf.* Fig. 6). However, the TPPP/p25-induced microtubule bundling was able to protect the microtubules from the depolymerization effect of the anti-microtubular agent (*cf.* Fig. 6). Thus, our results underline the previously proposed view, namely that the microtubules could not be stabilized by acetylation itself; rather other mechanisms could be responsible for this, and these stable microtubules then accumulate acetylated tubulins (22, 40). We propose that the expression of TPPP/p25, as a MAP (7, 41), could be a factor that induces the stabilization of the microtubule network via its bundling activity.

We also demonstrated that TPPP/p25 interacts with HDAC6 *in vitro*, and this interaction results in concentration-dependent inhibition of the HDAC6 deacetylase activity (*cf.* Fig. 4). This finding suggests that the heteroassociation of the two proteins leads to a successive acetylation of the microtubule network. A similar phenomenon has been reported for Tau, an important MAP of the central nervous system, which was found to inhibit HDAC6 deacetylase activity (with a maximum inhibition of 65%) (42), whereas TPPP/p25 resulted in virtually complete inhibition in the same concentration range. This new observation might imply innovative aspects because HDAC6 with its ubiquitous deacetylase activity is considered as a potential target of drugs for treating different human diseases (43–46).

Moreover, our finding that the interaction of TPPP/p25 and HDAC6 was reduced by the presence of tubulin, with the extent of the effect depending on the tubulin concentration and reaching practically complete inhibition at 1 μM tubulin concentration (*cf.* Fig. 4*B*), may suggest that HDAC6 and tubulin compete for the same binding "domain" of the unfolded TPPP/p25. Because TPPP/p25 has a similar sequence (**GS**HKERFD**P**S-**G**K**G**) with the tubulin binding domain of Tau (**GS**LGNIHHK-**PG**G**G**Q) and Tau interacts with HDAC6 with its microtubule binding domain (42), it can be hypothesized that the binding domain of TPPP/p25 to HDAC6 corresponds to its tubulin binding domain.

The role of tubulin acetylation in the dynamics of the microtubule system, a characteristic feature that is crucial for its physiological functions, has been extensively investigated because the dynamics of the microtubules enables the cells to rapidly reorganize the microtubule cytoskeleton in the course of cellular polarization, migration, and mitotic division (11–13). In these complex processes, both the decoration of the microtubules by the dynamic association of proteins (47) and the post-translational modifications play an important role (21, 22, 48). However, the molecular mechanisms of these events are not yet well defined (49–51). Therefore, the discovery of new MAPs could contribute to the further understanding of the reorganization of the microtubule system in physiological and pathological conditions. Here we showed that TPPP/p25 influences the microtubule growth velocity (*cf.* Fig. 8) as well as the microtubule-derived cell motility (*cf.* Fig. 9) by affecting the stability and the acetylation of the microtubules. Our present data suggest that the inhibitory effect of TPPP/p25 on the microtubule growth velocity could be related to its HDAC6-inhibitory activity because HDAC6 controls the microtubule dynamics via its interaction with the plus-end tip-binding proteins, an interaction that is prolonged by the presence of inhibitors, making the capping activity of HDAC6 more pronounced (37).

The change in the tubulin acetylation during the course of differentiation, myelination/migration of oligodendrocytes could be potentially important. We propose that TPPP/p25 controls the differentiation of oligodendrocytes via microtubule acetylation by inhibition of tubulin deacetylation; however, a possible activating effect on tubulin acetyltransferase(s) cannot be excluded and merits further experiments. Moreover, the TPPP/p25-induced microtubule stabilization by its bundling activity could also be essential for the maintenance of the projections of myelinating oligodendrocytes. In addition, the role of TPPP/p25 in cell motility could have a potentially important impact in remyelination as well as when oligodendrocyte progenitor cells need to migrate to their target destination *in vivo* (11).

Acknowledgment—We are grateful to Dr. Niels Galjart for providing the pGFP-EB3 construct.

REFERENCES

1. Takahashi, M., Tomizawa, K., Ishiguro, K., Sato, K., Omori, A., Sato, S., Shiratsuchi, A., Uchida, T., and Imahori, K. (1991) *FEBS Lett.* **289,** 37–43
2. Takahashi, M., Tomizawa, K., Fujita, S. C., Sato, K., Uchida, T., and Imahori, K. (1993) *J. Neurochem.* **60,** 228–235
3. Orosz, F., and Ovádi, J. (2008) *FEBS Lett.* **582,** 3757–3764
4. Kovács, G. G., László, L., Kovács, J., Jensen, P. H., Lindersson, E., Botond, G., Molnár, T., Perczel, A., Hudecz, F., Mezo, G., Erdei, A., Tirián, L., Lehotzky, A., Gelpi, E., Budka, H., and Ovádi, J. (2004) *Neurobiol. Dis.* **17,** 155–162
5. Kovács, G. G., Gelpi, E., Lehotzky, A., Höftberger, R., Erdei, A., Budka, H., and Ovádi, J. (2007) *Acta Neuropathol.* **113,** 153–161
6. Song, Y. J., Lundvig, D. M., Huang, Y., Gai, W. P., Blumbergs, P. C., Højrup, P., Otzen, D., Halliday, G. M., and Jensen, P. H. (2007) *Am. J. Pathol.* **171,** 1291–1303
7. Hlavanda, E., Kovács, J., Oláh, J., Orosz, F., Medzihradszky, K. F., and Ovádi, J. (2002) *Biochemistry* **41,** 8657–8664
8. Hlavanda, E., Klement, E., Kókai, E., Kovács, J., Vincze, O., Tökési, N., Orosz, F., Medzihradszky, K. F., Dombrádi, V., and Ovádi, J. (2007) *J. Biol. Chem.* **282,** 29531–29539
9. Lehotzky, A., Tirián, L., Tökési, N., Lénárt, P., Szabó, B., Kovács, J., and Ovádi, J. (2004) *J. Cell Sci.* **117,** 6249–6259
10. Lehotzky, A., Lau, P., Tokési, N., Muja, N., Hudson, L. D., and Ovádi, J. (2010) *Glia* **58,** 157–168
11. Bauer, N. G., Richter-Landsberg, C., and Ffrench-Constant, C. (2009) *Glia* **57,** 1691–1705
12. Tran, A. D., Marmo, T. P., Salam, A. A., Che, S., Finkelstein, E., Kabarriti, R., Xenias, H. S., Mazitschek, R., Hubbert, C., Kawaguchi, Y., Sheetz, M. P., Yao, T. P., and Bulinski, J. C. (2007) *J. Cell Sci.* **120,** 1469–1479
13. Reed, N. A., Cai, D., Blasius, T. L., Jih, G. T., Meyhofer, E., Gaertig, J., and Verhey, K. J. (2006) *Curr. Biol.* **16,** 2166–2172
14. Caceres, A., and Kosik, K. S. (1990) *Nature* **343,** 461–463
15. Takemura, R., Okabe, S., Umeyama, T., Kanai, Y., Cowan, N. J., and Hirokawa, N. (1992) *J. Cell Sci.* **103,** 953–964
16. MacRae, T. H. (1997) *Eur. J. Biochem.* **244,** 265–278
17. Westermann, S., and Weber, K. (2003) *Nat. Rev. Mol. Cell Biol.* **4,** 938–947
18. Fukushima, N., Furuta, D., Hidaka, Y., Moriyama, R., and Tsujiuchi, T. (2009) *J. Neurochem.* **109,** 683–693
19. Maruta, H., Greer, K., and Rosenbaum, J. L. (1986) *J. Cell Biol.* **103,** 571–579
20. Piperno, G., LeDizet, M., and Chang, X. J. (1987) *J. Cell Biol.* **104,** 289–302
21. Webster, D. R., and Borisy, G. G. (1989) *J. Cell Sci.* **92,** 57–65
22. Palazzo, A., Ackerman, B., and Gundersen, G. G. (2003) *Nature* **421,** 230
23. Yang, W. M., Yao, Y. L., Sun, J. M., Davie, J. R., and Seto, E. (1997) *J. Biol. Chem.* **272,** 28001–28007
24. Parmigiani, R. B., Xu, W. S., Venta-Perez, G., Erdjument-Bromage, H., Yaneva, M., Tempst, P., and Marks, P. A. (2008) *Proc. Natl. Acad. Sci. U.S.A.* **105,** 9633–9638
25. Nahhas, F., Dryden, S. C., Abrams, J., and Tainsky, M. A. (2007) *Mol. Cell Biochem.* **303,** 221–230
26. Li, W., Zhang, B., Tang, J., Cao, Q., Wu, Y., Wu, C., Guo, J., Ling, E. A., and Liang, F. (2007) *J. Neurosci.* **27,** 2606–2616
27. Ohkawa, N., Sugisaki, S., Tokunaga, E., Fujitani, K., Hayasaka, T., Setou, M., and Inokuchi, K. (2008) *Genes Cells* **13,** 1171–1183
28. Creppe, C., Malinouskaya, L., Volvert, M. L., Gillard, M., Close, P., Malaise, O., Laguesse, S., Cornez, I., Rahmouni, S., Ormenese, S., Belachew, S., Malgrange, B., Chapelle, J. P., Siebenlist, U., Moonen, G., Chariot, A., and Nguyen, L. (2009) *Cell* **136,** 551–564
29. Outeiro, T. F., Kontopoulos, E., Altmann, S. M., Kufareva, I., Strathearn, K. E., Amore, A. M., Volk, C. B., Maxwell, M. M., Rochet, J. C., McLean, P. J., Young, A. B., Abagyan, R., Feany, M. B., Hyman, B. T., and Kazantsev, A. G. (2007) *Science* **317,** 516–519
30. Dompierre, J. P., Godin, J. D., Charrin, B. C., Cordelières, F. P., King, S. J., Humbert, S., and Saudou, F. (2007) *J. Neurosci.* **27,** 3571–3583
31. Suzuki, K., and Koike, T. (2007) *Neuroscience* **147,** 599–612
32. Louis, J. C., Magal, E., Muir, D., Manthorpe, M., and Varon, S. (1992) *J. Neurosci. Res.* **31,** 193–204
33. Wang, S. Z., Dulin, J., Wu, H., Hurlock, E., Lee, S. E., Jansson, K., and Lu, Q. R. (2006) *Development* **133,** 3389–3398
34. Lim, A. C., Tiu, S. Y., Li, Q., and Qi, R. Z. (2004) *J. Biol. Chem.* **279,** 4433–4439

35. Tirián, L., Hlavanda, E., Oláh, J., Horváth, I., Orosz, F., Szabó, B., Kovács, J., Szabad, J., and Ovádi, J. (2003) *Proc. Natl. Acad. Sci. U.S.A.* **100,** 13976–13981
36. Vincze, O., Tökési, N., Oláh, J., Hlavanda, E., Zotter, A., Horváth, I., Lehotzky, A., Tirián, L., Medzihradszky, K. F., Kovács, J., Orosz, F., and Ovádi, J. (2006) *Biochemistry* **45,** 13818–13826
37. Zilberman, Y., Ballestrem, C., Carramusa, L., Mazitschek, R., Khochbin, S., and Bershadsky, A. (2009) *J. Cell Sci.* **122,** 3531–3541
38. Stepanova, T., Slemmer, J., Hoogenraad, C. C., Lansbergen, G., Dortland, B., De Zeeuw, C. I., Grosveld, F., van Cappellen, G., Akhmanova, A., and Galjart, N. (2003) *J. Neurosci.* **23,** 2655–2664
39. Haggarty, S. J., Koeller, K. M., Wong, J. C., Grozinger, C. M., and Schreiber, S. L. (2003) *Proc. Natl. Acad. Sci. U.S.A.* **100,** 4389–4394
40. Schulze, E., Asai, D. J., Bulinski, J. C., and Kirschner, M. (1987) *J. Cell Biol.* **105,** 2167–2177
41. Ovádi, J., and Orosz, F. (2009) *BioEssays* **31,** 676–686
42. Perez, M., Santa-Maria, I., Gomez de Barreda, E., Zhu, X., Cuadros, R., Cabrero, J. R., Sanchez-Madrid, F., Dawson, H. N., Vitek, M. P., Perry, G., Smith, M. A., and Avila, J. (2009) *J. Neurochem.* **109,** 1756–1766
43. Yoshida, M., Furumai, R., Nishiyama, M., Komatsu, Y., Nishino, N., and Horinouchi, S. (2001) *Cancer Chemother. Pharmacol.* **48,** Suppl. 1, S20–S26
44. Hideshima, T., Bradner, J. E., Wong, J., Chauhan, D., Richardson, P., Schreiber, S. L., and Anderson, K. C. (2005) *Proc. Natl. Acad. Sci. U.S.A.* **102,** 8567–8572
45. Kawada, J., Zou, P., Mazitschek, R., Bradner, J. E., and Cohen, J. I. (2009) *J. Biol. Chem.* **284,** 17102–17109
46. Jiang, Q., Ren, Y., and Feng, J. (2008) *J. Neurosci.* **28,** 12993–13002
47. Amos, L. A., and Schlieper, D. (2005) *Adv. Protein Chem.* **71,** 257–298
48. Hubbert, C., Guardiola, A., Shao, R., Kawaguchi, Y., Ito, A., Nixon, A., Yoshida, M., Wang, X. F., and Yao, T. P. (2002) *Nature* **417,** 455–458
49. Etienne-Manneville, S. (2004) *Traffic* **5,** 470–477
50. Basu, R., and Chang, F. (2007) *Curr. Opin. Cell Biol.* **19,** 88–94
51. Kawauchi, T., and Hoshino, M. (2008) *Dev. Neurosci.* **30,** 36–46